Numerical modelling of turbulent flow in a square river harbour

H. Hakimzadeh
Faculty of Civil Engineering, Sahand University of Technology, Iran.

Abstract

A two dimensional numerical hydrodynamic model including various turbulence models has been developed and applied to predict the stream induced circulation in a square river harbour. The turbulent flow was driven by a stationary current in an adjacent model river. Emphasis has been focused on comparing different turbulence models including: the depth-integrated mixing length, k-ε and algebraic stress models to predict accurately the velocity patterns within such basins. The finite difference method has been used to discretize the governing equations. For the solid boundaries the common no-slip boundary representation has been selected for the turbulent diffusion terms in the hydrodynamics equations. Moreover, the advective acceleration terms in the hydrodynamics equations were treated using the third order upwind scheme whereas the counterpart terms in the k-ε equations were treated using the exquisite scheme. The numerical model results have been compared with the experimental data and it was found that the k-ε and algebraic stress turbulence models generally produced the most accurate results for the tests considered within the harbour.

1 Introduction

The harbours situated along the rivers and estuaries usually suffer from siltation of their basins. Removal and disposal of sediments deposited in harbour basins often involve high cost, particularly when the sediment is contaminated with micro-pollutants that are adsorbed on the clay and silt particles. The siltation of a harbour results from a net transport of sediments into the harbour that is caused by the often quite complicated flow patterns in the harbour entrance. Since the siltation process mainly depends on the flow pattern, then the determination of

the velocity field within such basins will be an important issue. Software tools are now available to determine the flow pattern within such basins. A major requirement of these tools is that they can accurately predict the circulation pattern within such basins, before proceeding to predict the sedimentation process. However, such models are generally used for marina planning and are therefore rarely calibrated and verified against prototype data. On the other hand, the circulation patterns in harbour entrances driven by steady river flows have been extensively examined in the laboratory by a number of researchers. In the current study, data from experiments carried out by the hydromechanics group of the civil engineering faculty at the Delft University of Technology, Langendoen [1], (cited in Bijvelds et al. [2]) were used for model verification. These measurements concerned a stationary and homogeneous free surface cavity flow in a $1\times1m^2$ harbour. The flow in this model harbour was driven by a constant river discharge Q of $0.042m^3/s$; the water depth d equalled $0.11m$ at still water; and the width of the river was $1m$. The model river length was $5m$. The sidewalls of the model were vertical.

The numerical model results based on using the mixing length and k-ε model have already been compared with measured data and it was found that the k-ε turbulence was in good agreement with laboratory data, see Hakimzadeh [3]. For the numerical model reported herein, one of the most advanced turbulence models, i.e., the algebraic stress model, has been used for a square river harbour (see Figure 1).

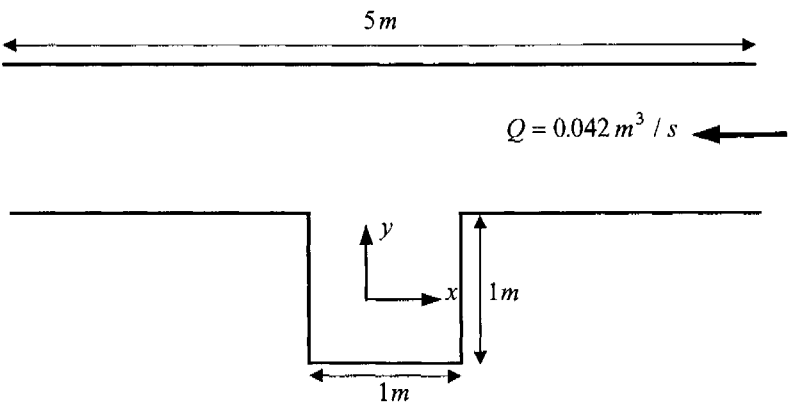

Figure 1: Configuration of the model harbour and river

2 Depth-integrated hydrodynamic equations

The equations of motion for a two-dimensional depth-averaged flow are best obtained by integrating the three-dimensional Reynolds equations over the depth. Assuming that the vertical acceleration is negligible compared to gravity, then the

continuity and horizontal equations can be derived as given by Falconer and Hakimzadeh [4]:

$$\frac{\partial \zeta}{\partial t}+\frac{\partial UH}{\partial x}+\frac{\partial VH}{\partial y}=0 \tag{1}$$

$$\frac{\partial UH}{\partial t}+\beta\left[\frac{\partial U^2H}{\partial x}+\frac{\partial UVH}{\partial y}\right]=f_cVH-gH\frac{\partial \zeta}{\partial x}+\frac{C_s\rho_aW_xW_s}{\rho},$$
$$-\frac{fUV_s}{2}+\frac{\partial(-\overline{u'u'})H}{\partial x}+\frac{\partial(-\overline{u'v'})H}{\partial y}. \tag{2}$$

$$\frac{\partial VH}{\partial t}+\beta\left[\frac{\partial UVH}{\partial x}+\frac{\partial V^2H}{\partial y}\right]=-f_cUH-gH\frac{\partial \zeta}{\partial y}+\frac{C_s\rho_aW_yW_s}{\rho},$$
$$-\frac{fVV_s}{2}+\frac{\partial(-\overline{v'u'})H}{\partial x}+\frac{\partial(-\overline{v'v'})H}{\partial y}. \tag{3}$$

where ζ = water surface elevation above (positive) datum, t = time, x,y = Cartesian co-ordinates in horizontal plane, U,V = depth averaged velocity components in x,y directions, H = total depth, β = momentum correction factor, f_c = Coriolis parameter (= $2\varpi\sin\phi$, where ϖ = speed of earth's rotation and ϕ = earth's latitude), g = gravity, C_s = air-water resistance coefficient, ρ_a = air density, ρ = fluid density, W_x, W_y = wind velocity components in x, y directions respectively, W_s = wind speed, f = Darcy bed friction factor, V_s = depth averaged fluid speed and $-\overline{u_i'u_j'}$ = the Reynolds stresses.

Assuming that the velocity profile in the vertical plane can be adequately represented by the logarithmic distribution, then the value of correction factor β for the non-uniformity of the velocity profile becomes:

$$\beta=1+1\Big/\left(\kappa\sqrt{2}\Big/\sqrt{f}-1\right)^2\cong 1+f/2\kappa^2 \tag{4}$$

where κ = von Karman's constant (=0.4). The Coriolis parameter and the wind stress were not included in the current study.

3 Turbulence models

In using the eddy viscosity concept, the Reynolds stresses have been represented as:

$$-\overline{u_i'u_j'}=\overline{\nu}_t\left(\frac{\partial U_i}{\partial x_j}+\frac{\partial U_j}{\partial x_i}\right)-\frac{2}{3}\bar{k}\delta_{ij} \tag{5}$$

The Kronecker delta δ_{ij} appearing in eqn (5) is equal to unity when $i = j$ and is zero when $i \neq j$. In applying the zero equation turbulence model, the turbulent eddy viscosity has been determined by the following equation [5]:

$$\bar{\nu}_t = 0.15 U_* H \tag{6}$$

where U_* = shear velocity

For the two-equation model, the depth integrated k-ε equations have been used to calculate the turbulent kinetic energy and dissipation rate, see Falconer and Li [6]:

$$\frac{\partial \bar{k} H}{\partial t} + \frac{\partial \bar{k} U H}{\partial x} + \frac{\partial \bar{k} V H}{\partial y} = \frac{\partial}{\partial x}\left(\frac{\bar{\nu}_t H}{\sigma_k} \cdot \frac{\partial \bar{k}}{\partial x}\right) + \frac{\partial}{\partial y}\left(\frac{\bar{\nu}_t H}{\sigma_k} \cdot \frac{\partial \bar{k}}{\partial y}\right),$$
$$+ \bar{\nu}_t H \left[2\left(\frac{\partial U}{\partial x}\right)^2 + 2\left(\frac{\partial V}{\partial y}\right)^2 + \left(\frac{\partial U}{\partial y} + \frac{\partial V}{\partial x}\right)^2 \right] + c_k U_*^3 - \bar{\varepsilon} H . \tag{7}$$

$$\frac{\partial \bar{\varepsilon} H}{\partial t} + \frac{\partial \bar{\varepsilon} U H}{\partial x} + \frac{\partial \bar{\varepsilon} V H}{\partial y} = \frac{\partial}{\partial x}\left(\frac{\bar{\nu}_t H}{\sigma_\varepsilon} \cdot \frac{\partial \bar{\varepsilon}}{\partial x}\right) + \frac{\partial}{\partial y}\left(\frac{\bar{\nu}_t H}{\sigma_\varepsilon} \cdot \frac{\partial \bar{\varepsilon}}{\partial y}\right),$$
$$+ c_{1\varepsilon} c_\mu \bar{k} H \left[2\left(\frac{\partial U}{\partial x}\right)^2 + 2\left(\frac{\partial V}{\partial y}\right)^2 + \left(\frac{\partial U}{\partial y} + \frac{\partial V}{\partial x}\right)^2 \right] + c_\varepsilon \frac{U_*^4}{H} - c_{2\varepsilon} \frac{\bar{\varepsilon}^2}{\bar{k}} H . \tag{8}$$

where $\bar{k}$ = turbulent kinetic energy, $\bar{\nu}_t$ = turbulent eddy viscosity, $\bar{\varepsilon}$ = dissipation rate of turbulent kinetic energy, $\sigma_k, \sigma_\varepsilon, c_\mu, c_{1\varepsilon}, c_{2\varepsilon}$ = constant coefficients, $c_k = (f/2)^{-1/2}$, $c_\varepsilon = 3.6 c_{2\varepsilon} c_\mu^{1/2} (f/2)^{-3/4}$, f = the Darcy friction factor and $\bar{\nu}_t = c_\mu \dfrac{\bar{k}^2}{\bar{\varepsilon}}$.

For the depth integrated algebraic stress model, the Reynolds stresses have been represented as [7]:

$$-\overline{u_i' u_i'} = 2A^2 B \left(\frac{\partial U_i}{\partial x_j}\right)^2 + 2A^2 P_{kv} \frac{\partial U_i}{\partial x_j} - 2AP_{kv} + B \tag{9}$$

$$-\overline{u_i' u_j'} = -AB \frac{\partial U_i}{\partial x_j} - AP_{kv} \tag{10}$$

where $A = \dfrac{1 - c_2}{c_1} \cdot \dfrac{\bar{k}}{\bar{\varepsilon}}$, $B = \dfrac{2\bar{k}}{3} \cdot \dfrac{1 - c_1 - c_2}{c_1}$, $P_{kv} = c_k \dfrac{U_*^3}{H}$ and $c_1 = 2.2, c_2 = 0.55$.

4 Boundary conditions

In the numerical model, the river flow boundaries were treated as open flow boundaries, with the river discharge set to be $0.042 m^3/s$. For an open boundary,

an inflow boundary condition was prescribed for the turbulent parameters, as suggested by Rodi [8]:

$$\bar{k} = \bar{\varepsilon} = 0 \tag{11}$$

For the turbulent parameters k and ε along a solid wall normal to the x-direction, the following assumption have been used [6]:

$$\frac{\partial \bar{k}}{\partial x} = 0 \text{ and } \frac{\partial \bar{\varepsilon}}{\partial x} = 0 \tag{12}$$

The turbulent characteristics adjacent to solid boundaries are calculated using a wall function approach [8], whereby:

$$\bar{k}_w = \frac{U_*^2}{c_\mu^{1/2}} \tag{13}$$

$$\bar{\varepsilon}_w = \frac{U_*^3}{\kappa z_c} \tag{14}$$

where z_c = distance from solid boundary. Details of the derivation of the wall function approach are given in Hakimzadeh [7].

Falconer and Hakimzadeh [4] have already investigated the influence of the different closed boundary representation on the predicted flow pattern within the model harbours. In the current study only the common no-slip boundary condition has been used for the velocity components.

5 Numerical method

In solving the governing equations, an alternating direction implicit finite difference scheme has been used, including a refined and more accurate space staggered grid scheme where depths are included at the centre of grid sides. A rectangular grid of cell size $25mm \times 25mm$ was chosen, with the computational domain therefore containing 200×82 grid cells. The difference equations were fully centred in both time and space, with the advective acceleration and the turbulent diffusion terms being centred by iteration. The difference scheme had no stability constraints, although it was established that the accuracy of the scheme deteriorated rapidly when the Courant number exceeded about eight. In the finite difference equations, particular attention was paid to the treatment of the advective acceleration terms, with these terms being of considerable importance in modelling re-circulating flows. The components of the advective accelerations were represented in their pure differential form, thereby conserving momentum precisely in the difference scheme. These terms were also represented using the higher order accurate third order upwind scheme, which eliminates the introduction of numerical diffusion and minimises grid scale oscillations. On the other hand, the counterpart terms in the depth integrated k-ε equations were represented using the exquisite scheme, as proposed by Leonard [9].

6 Model results and comparisons

At the open boundaries the rate of flow was started from zero, increased on a sine curve up to a certain value (i.e. the river discharge) and then was remained constant. Therefore, a circulation cell grew rapidly in strength and shape within the model harbour and then it became stable.

For the numerical model predictions the velocity distribution were somewhat similar within the basin in using the three turbulence models and the large eddy dominated within the model harbour. The mixing length model often predicted a slightly different flow structure from that obtained using the k-ε or algebraic stress turbulence models. However, in using improved turbulence models such as the k-ε and algebraic stress models, there was no significant difference in the predicted numerical results. Figure 2a illustrates the predicted circulation pattern within the harbour using the mixing length turbulence model. In applying this model with the no-slip-closed boundary condition the values of velocities adjacent to the wall were under-predicted. Figure 2b illustrates the predicted circulation pattern within the harbour using the k-ε turbulence model. As can be seen from the figure, the predicted circulation cell of the k-ε model seems to be more accurate than that of the mixing length model.

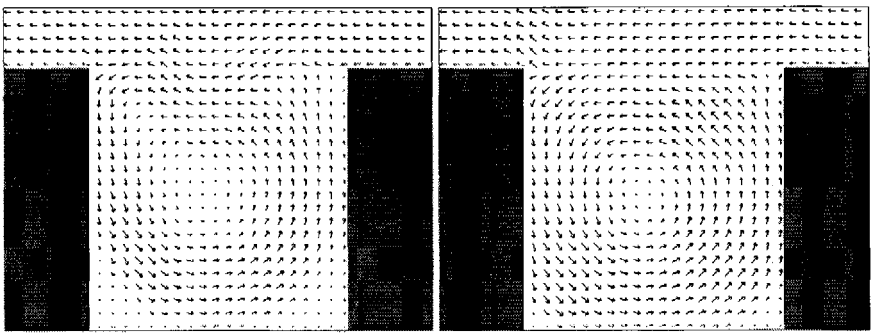

a) the mixing length model b) the k-ε model

Figure 2: Flow pattern within the harbour using two different turbulence models

Also, figure 3a shows the calculated eddy viscosity distribution using the mixing length model within the model harbour. As can be seen from this figure, the minimum and maximum values of the isolines of horizontal eddy viscosity in the model harbour were about $30mm^2/s$ and $100mm^2/s$, respectively. Similarly, figure 3b shows the predicted eddy viscosity distribution using the k-ε model within the model harbour. It can be seen from this figure, and in contrast to the previous model predictions, the minimum and maximum values of the isolines of horizontal eddy viscosity in the harbour were about $100mm^2/s$ and $900mm^2/s$, respectively.

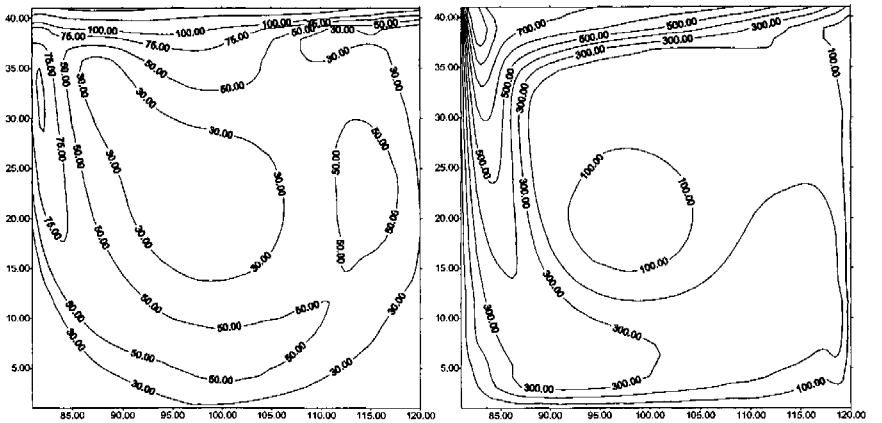

a) the mixing length turbulence model b) the k-ε turbulence model

Figure 3: Eddy viscosity distribution within the harbour (mm^2/s)

The predicted circulation pattern within the harbour using the algebraic stress turbulence model is shown in figure 4. It can be seen from this figure that the predicted circulation cell within the harbour is similar to that of the k-ε model. However, the numerical model results are slightly different from those predicted with the k-ε model. Also, the predicted turbulent kinetic energy and the normal Reynolds stress distributions using the algebraic stress model within the basin are shown in figures 5 and 6, respectively. For the current tests both the k-ε and algebraic stress models with a no-slip-closed boundary condition, have correctly predicted the large eddy and which is in good agreement with the laboratory measurements.

Another typical example of comparisons between the measured and numerically predicted results for the different turbulence models is illustrated in figures 7a and 7b, where the 'V ' and 'U' velocity profiles across the two main axes are shown respectively. As can be seen from these comparisons, the predicted velocity values of the mixing length model were under-estimated whereas the predicted values of the sophisticated turbulence models were in good agreement with the experimental data. In comparing all of the velocity results it was found that the k-ε and algebraic turbulence models generally produced accurate results for all of the tests considered.

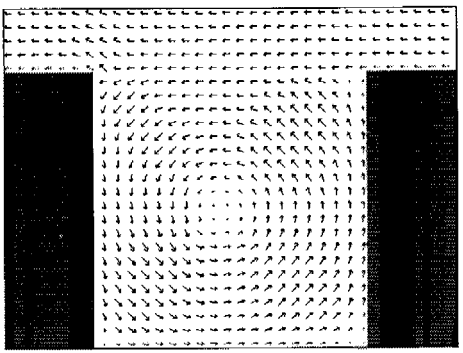

Figure 4: Flow pattern within the harbour using the algebraic stress model

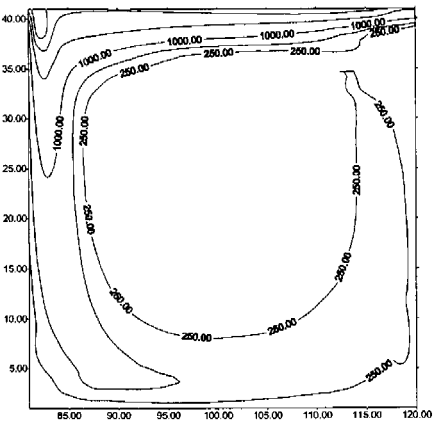

Figure 5: Turbulent kinetic energy distribution using the algebraic stress model

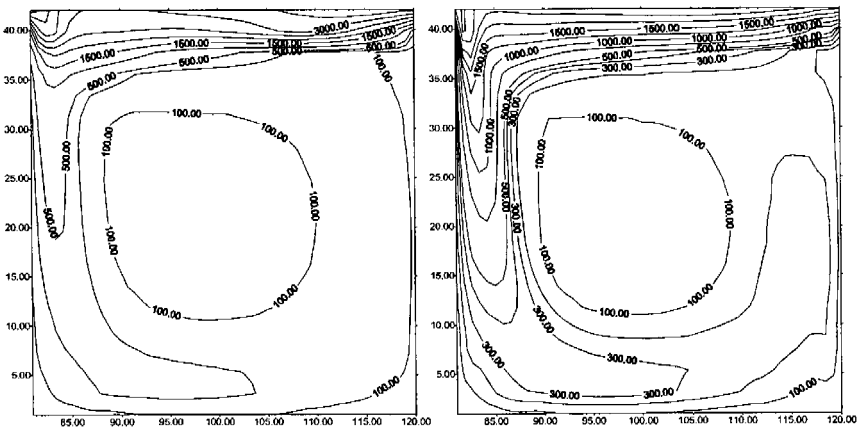

a) $u'u'$ b) $v'v'$

Figure 6:Reynolds stress distribution using the algebraic stress model (mm^2 / s^2)

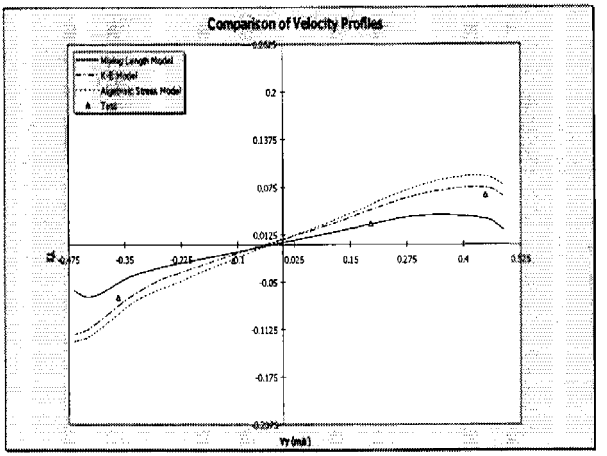

Figure 7a: Comparison of velocity profile across the x axis

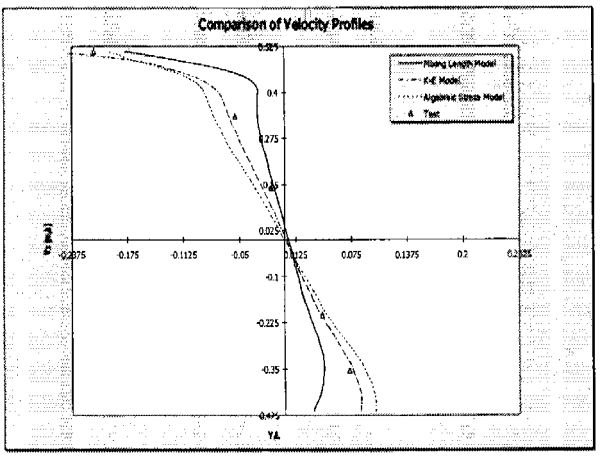

Figure 7b: Comparison of velocity profile across the y axis

7 Conclusion

Details are given of an extensive ongoing research programme to predict more accurately the circulation cell within the river harbours. In the study reported herein three different turbulence models have been considered, including the depth-integrated simple mixing length model, k-ε and algebraic stress models. The findings from this study have shown that the numerical model results of the mixing length model were under-predicted. In contrast, the k-ε and algebraic stress models have reproduced the circulation cell and the velocity field very accurately for the harbour and these model are therefore recommended for

modelling cavity turbulent flow and circulation patterns in marinas and harbours. The eddy viscosity values predicted using the two-equation turbulence model were generally larger than those predicted using a simple mixing length turbulence model. Although the disparate eddy viscosity distributions obtained using the k-ε and the simple mixing length turbulence models showed little difference in terms of the velocity field predictions, the effect was expected to be much more pronounced on the turbulent diffusion of conservative and non-conservative solute distributions.

8 Acknowledgements

The numerical model study presented herein was a part of an ongoing research programme funded by Sahand University of Technology. The author received much assistance from the research committee of the university and is grateful for their co-operation.

References

[1] Langendoen, E.J. "Flow patterns and transport of dissolved matter in tidal harbours", *PhD Thesis,* Delft University of Technology, Delft, The Netherlands, 1992.

[2] Bijvelds, M.D.J.P., Kranenburg, C. and Stelling, G.S. "3D Numerical Simulation of Turbulent Shallow-Water Flow in Square Harbour", *Journal of Hydraulic Engineering.,* Vol. 125, No.1, pp. 26-31, 1999.

[3] Hakimzadeh, H. "Numerical Modelling of Cavity Flow in a Square Harbour Using the k-ε Turbulence Model", *Proceedings of International Conference on Hydraulic Structures*, Kerman, Iran, Vol. 3, pp. 31-40, 2001.

[4] Falconer, R.A. and Hakimzadeh, H. "Numerical modelling of secondary tide induced circulation in rectangular harbours with large aspect ratios" *Proceedings of Third International Conference on Planning, Design and Operation of Marinas,* ed. W.R. Blain, Computational Mechanics Publications, pp. 109-118, 1995.

[5] Fischer, H.B. "Longitudinal Dispersion and Turbulent Mixing in Open Channel Flow", *Annual Review of Fluid Mechanics,* 5, pp. 59-78, 1973.

[6] Falconer, R.A. and Li, G. "Numerical modelling of tidal eddies in coastal basins with narrow entrances using the k-ε turbulence model" in *Mixing and Transport in the Environment,* eds. K.J. Beven, et. al., John Wiley & Sons Ltd., London, pp. 325-350, 1994.

[7] Hakimzadeh, H. "Turbulence Modelling of Tidal Currents in Rectangular Harbours", PhD Thesis, University of Bradford, Bradford, UK, 1997.

[8] Rodi, W. "Turbulence Models and their Application in Hydraulics", *IAHR,* Second Edition, Delft, The Netherlands, pp. 1-104, 1984.

[9] Leonard, B.P. "Elliptic systems: finite difference method IV" *Handbook of Numerical Heat Transfer,* eds. W.J.Minkowichz, et. al. Wiley, New York, Chapter 9, pp. 347-378, 1988.